## Title
Methods for monitoring erosion using optical coherence tomography



Authors
Chan, Kenneth H
Chan, Andrew C
Darling, Cynthia L
et al.

Publication Date
2013-03-25

DOI
10.1117/12.2011013

Peer reviewed

HHS Public Access
Author manuscript
*Proc SPIE Int Soc Opt Eng*. Author manuscript; available in PMC 2014 January 22.

Published in final edited form as:
*Proc SPIE Int Soc Opt Eng*. 2013 March 25; 8566: 856606–. doi:10.1117/12.2011013.

# Methods for Monitoring Erosion Using Optical Coherence Tomography

**Kenneth H. Chan**, **Andrew C. Chan**, **Cynthia L. Darling**, and **Daniel Fried**[1]
University of California, San Francisco, San Francisco, CA 94143-0758

## Abstract

Since optical coherence tomography is well suited for measuring small dimensional changes on tooth surfaces it has great potential for monitoring tooth erosion. The purpose of this study was to explore different approaches for monitoring the erosion of enamel. Application of an acid resistant varnish to protect the tooth surface from erosion has proven effective for providing a reference surface for *in vitro* studies but has limited potential for *in vivo* studies. Two approaches which can potentially be used *in vivo* were investigated. The first approach is to measure the remaining enamel thickness, namely the distance from the tooth surface to the dentinal-enamel junction (DEJ). The second more novel approach is to irradiate the surface with a carbon dioxide laser to create a reference layer which resists erosion. Measuring the remaining enamel thickness proved challenging since the surface roughening and subsurface demineralization that commonly occurs during the erosion process can prevent resolution of the underlying DEJ. The areas irradiated by the laser manifested lower rates of erosion compared to the non-irradiated areas and this method appears promising but it is highly dependent on the severity of the acid challenge.

### Keywords

erosion; optical coherence tomography; caries prevention; carbon dioxide laser

## 1. INTRODUCTION

Since optical coherence tomography is capable of measuring dimensional changes nondestructively on tooth surfaces it appears to be an ideal tool for monitoring tooth erosion. Dental erosion refers to the removal and softening of tooth surfaces due to a variety of factors and it often involves subsurface demineralization[1]. Several studies have demonstrated that polarization sensitive optical coherence tomography (PS-OCT) can be used to nondestructively measure the severity of subsurface demineralization in enamel and dentin and is therefore well suited for this role [2-14]. Early *in vitro* studies of the use of OCT for monitoring tooth demineralization demonstrated that OCT can be used to measure the loss of enamel due to exposure to a demineralizing solution. In the study of Fried et al.[15], acid resistant varnish was added to a control surface and this surface served as a reference surface to quantify the loss of enamel exposed to erosion. Although this approach is simple


[1]daniel.fried@ucsf.edu.

to implement *in vitro*, more robust adhesives such as composites would be needed in order to employ it *in vivo* and they would have to be employed in areas that are not subject to wear. One can also achieve the inhibition of demineralization and erosion via laser irradiation[16-18]. In previous studies investigating the use of optical coherence tomography for quantifying the severity of tooth demineralization, we discovered that areas of enamel peripheral to reference marks cut into enamel surfaces manifested increased resistance to erosion. In our dissolution studies on human and bovine enamel blocks we produced laser incisions to separate the groups (Fig. 1). In certain demineralization models we investigated, surface erosion occurred as opposed to the desired formation of subsurface lesions. We noticed that the areas irradiated by the laser were preferentially protected and those areas were not eroded but were left protruding from the surface[19]. Based on these observations, we hypothesized that select areas on tooth surfaces can be irradiated with the laser to reduce the erosion rate and serve as reference surfaces to estimate the rate of erosion.

Monitoring the remaining enamel thickness can also be used as an indicator of erosion. Wilder-Smith et al. [20]carried out an *in vivo* study of erosion caused by GastroEsophageal Reflux Disease (GERD) and they were able to measure very small rates of erosion. There are many challenges in accurately measuring the remaining enamel thickness. The dentinal enamel junction (DEJ) is scalloped and does not present a sharp boundary[21]. If erosion is accompanied by subsurface demineralization or roughens the surface, the strong increase in scattering interferes with the ability to resolve the DEJ. The tooth surface is often covered by a layer of saliva and the thickness of that layer can vary causing additional variation in the optical path length. The purpose of this study was to explore these methods to determine if they have potential for monitoring tooth erosion *in vivo*.

## 2. MATERIALS AND METHODS

### Sample Preparation and Erosion Models

**Laser Irradiated Surface (Protected Surface) Model—**Twenty bovine enamel blocks, approximately 8–12 mm in length, 2-mm in width, and a thickness of ~1 mm of bovine enamel were prepared from extracted tooth incisors acquired from a slaughterhouse. Each enamel sample was partitioned into six regions or windows (two sound enamel and four demineralization areas) by etching 140 $\mu$m wide incisions 1.4-mm apart across each of the enamel blocks using a laser (see Fig. 1). Incisions were etched using a transverse excited atmospheric pressure (TEA) $CO_2$ laser operating at 9.3 $\mu$m with a fluence of 200 J/cm$^2$, Impact 2500, GSI Lumonics (Rugby, U.K.). The high fluence was used to mimic results presented in a previous study [19] and to also demarcate the laser-irradiated area. The laser irradiated area also has increased resistance to acid dissolution which protects the region from further demineralization and erosion. This laser-irradiated surface can serve as a reference point for measuring the amount of erosion. A thin layer of acid resistant varnish, red nail polish, Revlon (New York, NY) was applied to protect the sound enamel control area on each end of the block. Samples were split into two groups of ten samples each and exposed to a pH cycling model of either 4.3 or 4.5 pH demineralization solution composed of a 40-ml aliquot of 2.0 mmol/L calcium, 2.0 mmol/L phosphate, and 0.075 mol/L acetate followed up with a 7.0 pH remineralization solution composed of a 40-ml aliquot of 1.5

mmol/L calcium, 0.9 mmol/L phosphate, 150 mmol/L potassium chloride, and 20 mmol/L cacodylate. The pH cycle was repeated for intervals of 3 times (3, 6, 9, 12 pH cyclings) for each window.

Ten blocks were exposed to a daily pH cycling regimen consisting of immersion in a demineralization solution ( pH 4.3 ) for 6 h, followed by a rinse with de-ionized water, and immersion in a remineralization solution (pH 7.0) for 17 h at 37°C. After every 3 pH cycles, a window was covered with a thin layer of acid resistant varnish to prevent further demineralization. This pH cycling was repeated for 12 days. After the 12 days, the samples were stored in 0.1% thymol solution to prevent fungal and bacterial growth. The remaining ten blocks were identical to the previous pH cycling, but instead experienced a weaker acid challenge in a 4.5 pH demineralization solution.

After the pH cycling was completed, the acid resistant varnish was removed with acetone, Fisher Scientific (Hampton, New Hampshire). Optical Coherence Tomography (OCT) scans were taken to assess the amount of erosion that had taken place by comparing the heights of the demineralized windows and laser-irradiated regions to the surface protected ends of the sample.

**Remaining Enamel Thickness - (DEJ) Model—**Sound whole incisors taken from teeth extracted from patients in the San Francisco Bay Area were collected, cleaned, and sterilized with gamma radiation. Twenty buccal hemisectioned human incisors were prepared with the roots cut off below the cementoenamel junction. Each sample was coated with a thin acid resistant varnish in the form of a red nail polish, Revlon (New York, NY) with the exception of a rectangular 2-mm wide region running along the occlusal-cervical direction on the buccal surface (see Fig. 2). Surface softened lesions were generated using the same demineralization solution (pH 4.3) described above. Orange juice was used which is highly acidic and is commonly used as an erosive agent for *in vitro* studies. The pH of the orange juice was measured to be 3.8.

Ten hemisectioned incisors were placed into the demineralization solution for 12 h at 37°C and the other ten samples were placed into orange juice under the same conditions. After every 12 h, the samples were scanned using a polarization-sensitive optical coherence tomography system (PS-OCT). It was determined at this time that the surface of the samples was drying out, dramatically increasing surface scattering which prevented resolution of the DEJ. We therefore switched to acquiring only individual b-scan images as opposed to complete 3D tomograms to speed acquisition and prevent the surfaces from drying. Further scans were acquired at 36 h and 48 h time points. The reduced attenuation provided by the wet surfaces allowed better resolution of the dentin-enamel junction. After 48 h demineralization, samples were stored in 0.1% thymol solution for sample preservation.

**PS-OCT System—**An all-fiber-based optical coherence domain reflectometry (OCDR) system with polarization maintaining (PM) optical fiber, high-speed piezoelectric fiber-stretchers and two balanced InGaAs receivers that was designed and fabricated by Optiphase, Inc., Van Nuys, CA. This two-channel system was integrated with a broadband superluminescent diode (SLD) Denselight (Jessup, MD) and a high-speed XY-scanning system (ESP 300 controller and 850G-HS stages, National Instruments, Austin, TX) for *in vitro* optical tomography. This system is based on a polarization-sensitive Michelson white light interferometer. The high power (15 mW) polarized SLD source operated at a center wavelength of 1317 nm with a spectral bandwidth full-width at half-maximum (FWHM) of 84 nm was aligned using polarization controller to deliver 15 mW into the slow axis of the PM fiber of the source arm of the interferometer. This light was split into the reference and sample arms of the Michelson interferometer by a 50/50 PM-fiber coupler. The sample arm was coupled to an AR-coated fiber-collimator to produce a 6-mm in diameter, collimated beam. That beam was focused onto the sample surface using a 20-mm focal length AR-coated planoconvex lens. This configuration provided lateral resolution of approximately 20 $\mu$m and an axial resolution of 10 $\mu$m in air with a signal to noise ratio of greater than 40–50 dB. The PS-OCT system is completely controlled using Labview software (National Instruments, Austin, TX). The system is described in greater detail in reference [6]. Acquired scans are compiled into *b-scan* files. Image processing was carried out using Igor Pro, data analysis software (Wavemetrics Inc., Lake Oswego, OR).

**Analysis of Erosion rates from OCT Scans—**Surface and DEJ measurements were done using the parallel-axis OCT scans acquired from the PM fiber-based PS-OCT to determine the heights of both laser-irradiated and remaining surface-DEJ thickness models. In the laser-irradiated model, heights in each laser-irradiated zone and demineralized window were compared with the control window at each end of the sample. The remaining surface-DEJ thickness was calculated through visual assessment of the entire *b-scan* in the majority of cases the DEJ was not identifiable in individual a-scans. If the DEJ was apparent, the distance between the surface and DEJ was recorded at a location of 2.5-mm above the CEJ (Fig. 3). Sample groups were compared using repeated measures analysis of variance (RM-ANOVA) with a Tukey–Kramer *post hoc* multiple comparison test. Prism from GraphPad software (San Diego, CA) was used for statistical calculations.

## 3. RESULTS AND DISCUSSION

Two OCT b-scans of samples with the reference marks cut with the carbon dioxide laser after exposure to the demineralization solutions at 4.3 and 4.5 pH are shown in Fig. 2. The Gaussian spatial profile of the $CO_2$ laser pulses produced a central incision approximately 50-$\mu$m deep along with areas on both sides of the incision (the “wings”) where the fluence was below the ablation threshold but still imparted protection against erosion. Figure 2A shows that the nonablative wings retained the acid resistant properties of the laser irradiated enamel surfaces, and when compared to the acid resistant protected windows at the ends of the sample, manifested little to no erosion. However at the higher acid challenge of 4.3 pH demineralization (Fig. 2B), there was some erosion of the laser-irradiated edges along with the untreated enamel windows, but the laser treated surfaces still inhibited erosion compared to the untreated areas. These results suggest that it may be feasible to utilize these laser-irradiated (protected) areas to monitor erosion, however the effectiveness of this is highly dependent on the demineralization model. If the model is too severe, it will etch away the laser markings. It is important to note that the laser treated surfaces appeared quite effective in inhibiting the surface loss in these somewhat severe demineralization models. It is also important to note that bovine enamel is more susceptible to demineralization and erosion than human enamel. We plan to further investigate this approach using different erosion models and with laser surface treatments at subablative fluence.

The other method for monitoring erosion investigated in this study involved measurement of the remaining enamel thickness, i.e., the distance from the tooth surface to the DEJ via analysis of the OCT b-scans. Figure 3 shows an OCT b-scan cross-section of an incisor before and after 12 hours of exposure to the demineralization solution with a pH of 4.3. After exposure to 12 hours of demineralization, sample surfaces began to roughen markedly reducing the optical penetration. Figure 3B shows that after 12 hours of demineralization, the DEJ was not resolvable using OCT due to the drop in optical penetration from the increased backscattering caused by surface demineralization.

After 24 hours demineralization at 4.3 pH and with orange juice (pH 3.8) the DEJ was no longer visible for any of the samples. We discovered that in the time it took to acquire entire 3D images with our OCT system, the sample surfaces dried sufficiently to further reduce optical penetration. As stated earlier for the remaining scans at 36 and 48 hours, the scans were rapidly acquired to prevent dehydration of the surfaces. Following this procedure a few of the samples regained DEJ visibility by maintaining better hydration of the surfaces, as shown in Figure 4. It appears the wet surface is important for improving index matching of the rough eroded surface to reduce surface scattering. Out of the 20 samples initially scanned with OCT, only 6 samples, maintained visibility of the DEJ as shown in Figure 5. The visibility of the DEJ declined exponentially as the demineralization continued over an interval of 12 hours. Of the 6 remaining samples with their DEJ visible, 3 from each demineralization group, the surface to DEJ distance was calculated. This method of measuring the surface to DEJ proved to be unreliable as the groups' mean distance actually increased at 48 hours of demineralization and resolving the DEJ was also of concern.

We have identified several limitations regarding monitoring the remaining enamel thickness for determining the rate of erosion. Tooth surfaces, particularly actively eroding surfaces may be rough and not perfectly flat; and this coupled with the fact that the DEJ may not present a sharp demarcation makes it very challenging to measure the remaining enamel thickness. This is further complicated by the strong attenuation that may occur from scattering from the roughened surface and any subsurface erosion that occurs. Maintaining hydration is critical to reducing that attenuation, however a layer of water or saliva on the surface will also influence the optical path length and the measurement of the remaining enamel thickness. Regarding the *in vivo* study of Wilder-Smith et al. [20], they do not comment on any problems mentioned above and the images of the eroded surfaces presented in the paper appear perfectly smooth with no roughening or subsurface demineralization visible.

## 4. ACKNOWLEDGMENTS

This work was supported by NIH/NIDCR Grants R01-DE17869.

## 5. REFERENCES

1. Lussi, A., editor. Dental Erosion:From Diagnosis to Therapy. KARGER; New York: 2006.

2. Baumgartner A, Dicht S, Hitzenberger CK, Sattmann H, Robi B, Moritz A, Sperr W, Fercher AF. Polarization-sensitive optical optical coherence tomography of dental structures. Caries Res. 2000; 34:59–69. [PubMed: 10601786]
3. Wang XJ, Milner TE, de Boer JF, Zhang Y, Pashley DH, Nelson JS. Characterization of dentin and enamel by use of optical coherence tomography. Applied Optics. 1999; 38(10):2092–2096. [PubMed: 18319769]
4. Everett MJ, Colston BW, Sathyam US, Silva LBD, Fried D, Featherstone JDB. Non-invasive diagnosis of early caries with polarization sensitive optical coherence tomography (PS-OCT). SPIE Proceeding. 1999; 3593:177–183.
5. Feldchtein FI, Gelikonov GV, Gelikonov VM, Iksanov RR, Kuranov RV, Sergeev AM, Gladkova ND, Ourutina MN, Warren JA, Reitze DH. In vivo OCT imaging of hard and soft tissue of the oral cavity. Optics Express. 1998; 3(3):239–251. [PubMed: 19384366]
6. Fried D, Xie J, Shafi S, Featherstone JDB, Breunig T, Lee CQ. Early detection of dental caries and lesion progression with polarization sensitive optical coherence tomography. J. Biomed. Optics. 2002; 7(4):618–627.
7. Jones RS, Fried D. Remineralization of enamel caries can decrease optical reflectivity. Journal of dental research. 2006; 85(9):804–808. [PubMed: 16931861]
8. Ngaotheppitak P, Darling CL, Fried D. Polarization Optical Coherence Tomography for the Measuring the Severity of Caries Lesions. Lasers Surg Med. 2005; 37(1):78–88. [PubMed: 15889402]
9. Jones RS, Darling CL, Featherstone JD, Fried D. Remineralization of in vitro dental caries assessed with polarization-sensitive optical coherence tomography. Journal of Biomedical Optics. 2006; 11(1):014016. [PubMed: 16526893]
10. Lee C, Darling C, Fried D. Polarization Sensitive Optical Coherence Tomographic Imaging of Artificial Demineralization on Exposed Surfaces of Tooth Roots. Dent. Mat. 2009; 25(6):721–728.
11. Manesh SK, Darling CL, Fried D. Nondestructive assessment of dentin demineralization using polarization-sensitive optical coherence tomography after exposure to fluoride and laser irradiation. J Biomed Mater Res B Appl Biomater. 2009; 90(2):802–812. [PubMed: 19283826]
12. Manesh SK, Darling CL, Fried D. Polarization-sensitive optical coherence tomography for the nondestructive assessment of the remineralization of dentin. Journal of Biomedical Optics. 2009; 14(4):044002. [PubMed: 19725714]
13. Louie T, Lee C, Hsu D, Hirasuna K, Manesh S, Staninec M, Darling CL, Fried D. Clinical assessment of early tooth demineralization using polarization sensitive optical coherence tomography. Lasers in Surgery and Medicine. 2010; 42(10):738–745. [PubMed: 21246578]
14. Staninec M, Douglas SM, Darling CL, Chan K, Kang H, Lee RC, Fried D. Nondestructive Clinical Assessment of Occlusal Caries Lesions using Near-IR Imaging Methods. Lasers in Surgery and Medicine. 2011; 43(10):951–959. [PubMed: 22109697]
15. Fried D, Xie J, Shafi S, Featherstone JD, Breunig TM, Le C. Imaging caries lesions and lesion progression with polarization sensitive optical coherence tomography. Journal of Biomedical Optics. 2002; 7(4):618–627. [PubMed: 12421130]
16. Featherstone JD, Barrett-Vespone NA, Fried D, Kantorowitz Z, Seka W. $CO_2$ laser inhibitor of artificial caries-like lesion progression in dental enamel. Journal of dental research. 1998; 77(6): 1397–1403. [PubMed: 9649168]
17. Fried D, Featherstone JD, Le CQ, Fan K. Dissolution studies of bovine dental enamel surfaces modified by high-speed scanning ablation with a $\lambda = 9.3\text{-}\mu m$ TEA $CO_2$ laser. Lasers in Surgery and Medicine. 2006; 38(9):837–845. [PubMed: 17044095]
18. Zuerlein MJ, Fried D, Featherstone JD. Modeling the modification depth of carbon dioxide laser-treated dental enamel. Lasers in Surgery and Medicine. 1999; 25(4):335–347. [PubMed: 10534750]
19. Le MH, Darling CL, Fried D. Automated analysis of lesion depth and integrated reflectivity in PS-OCT scans of tooth demineralization. Lasers in Surgery and Medicine. 2010; 42(1):62–68. [PubMed: 20077486]
20. Wilder-Smith CH, Wilder-Smith P, Kawakami-Wong H, Voronets J, Osann K, Lussi A. Quantification of Dental Erosions in Patients With GERD Using Optical Coherence Tomography

Before and After Double-Blind, Randomized Treatment With Esomeprazole or Placebo. Am J Gastroenterol. 2009; 104:2788–2795. [PubMed: 19654570]

21. Nanci, A. Ten Cate's Oral Histology: Development, Structure, and Function. Mosby; New York: 2007. 7e

**Fig. 1.**
Laser irradiated model (25x)

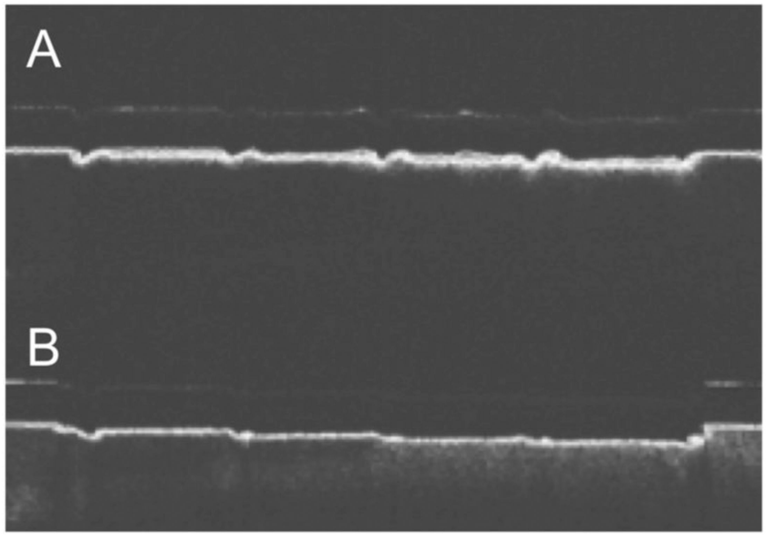


**Fig. 2.**
Laser irradiated model shows the irradiated zones to be resistant to some degree to the acid challenge. The irradiated zones are highly dependent of the acid challenge, for example, the 4.3 pH demineralization (B) showed to erode a lot more of the fiducil markings than the 4.5 pH (A).

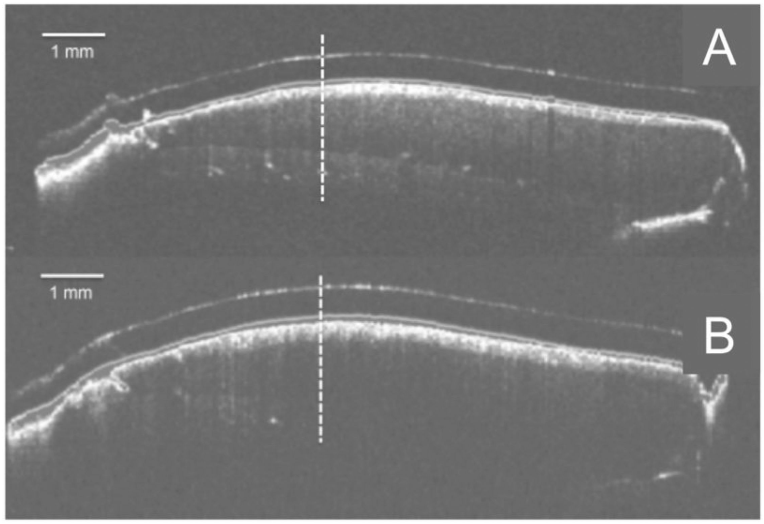


**Fig. 3.**
OCT *b-scan* of an incisor used in the remaining enamel thickness model at a pH of 4.3. Dotted white line demarcates where the DEJ was measured at a distance of 2.5-mm from the CEJ. (A) Initial OCT scan showing the DEJ structure. (B) After 12 hours of 4.3 pH demineralization, DEJ is irresolvable.

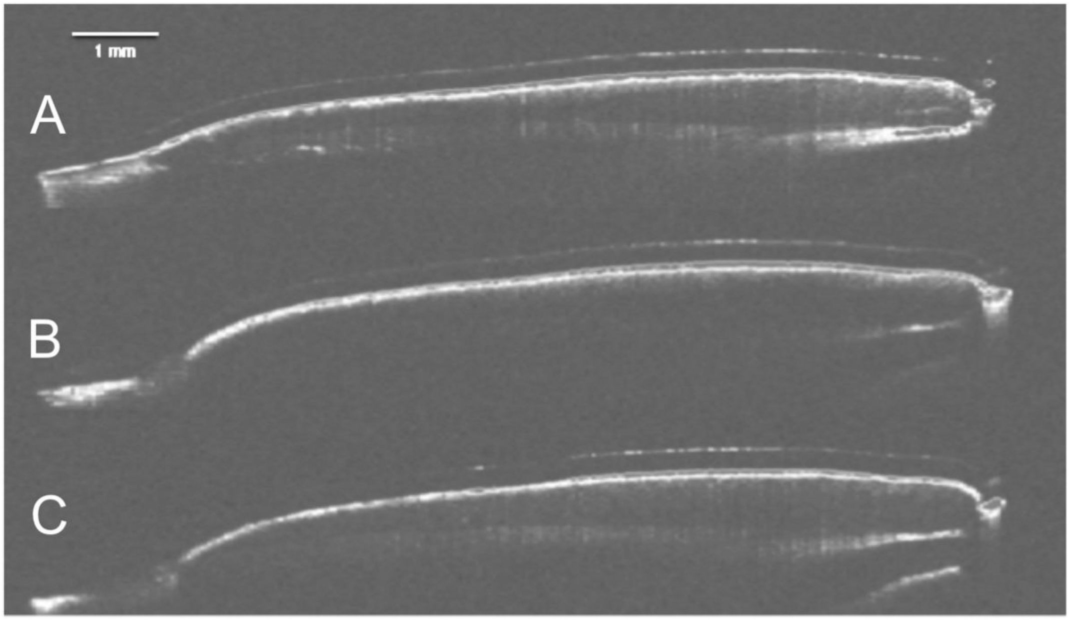


**Fig. 4.**
Parallel-axis OCT scans of the remaining surface-DEJ model over periods of demineralization at 4.3 pH and when the surface was wetted. (A) Initial scan, (B) 24 h demin, and (C) 36 h demin. The DEJ resurfaces in the OCT scan (C) when the surface was wetted.

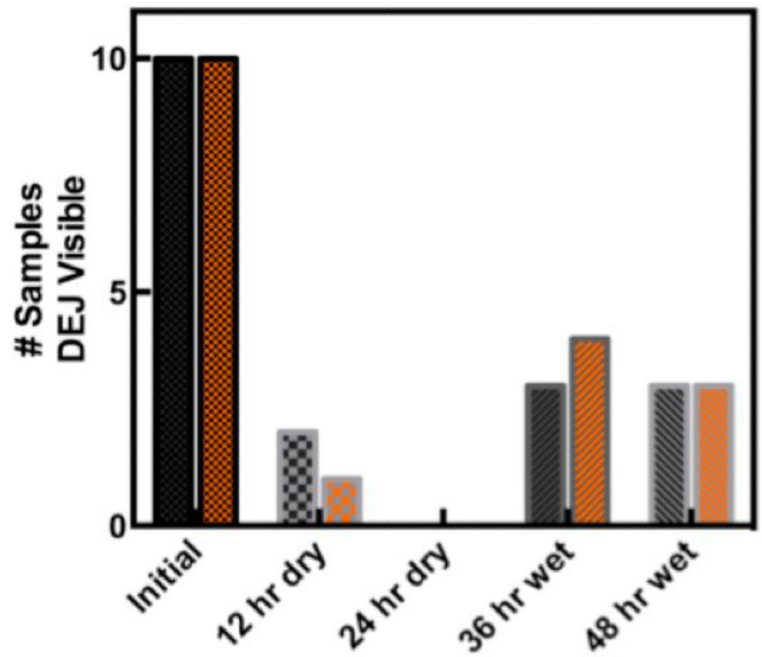


**Fig. 5.**
Visibility of DEJ among the samples over a period of demineralization and surface wetness.

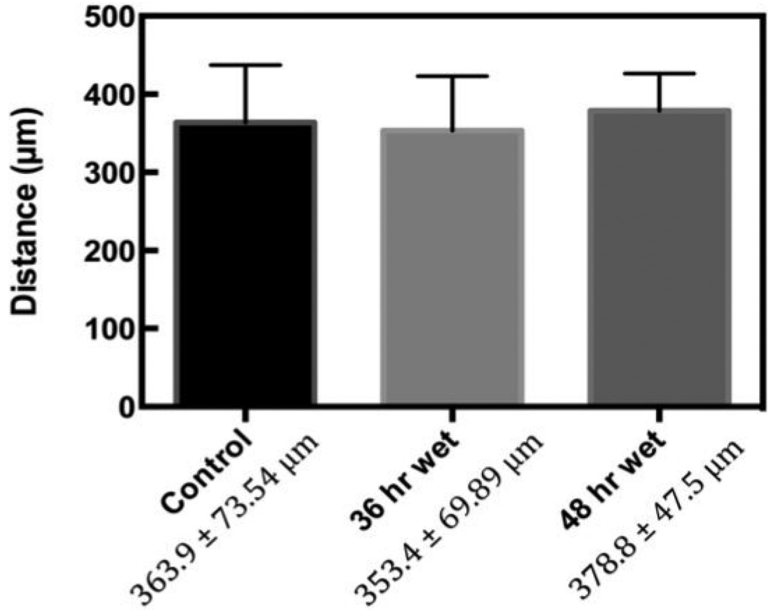


**Fig. 6.**

Plot of the mean ± S.D. of DEJ depth for the wet surface samples that the DEJ were visible in 48 hr.